Contrib Mineral Petrol (1986) 94:427–437

Contributions to Mineralogy and Petrology

Four zircon ages from one rock: the history of a 3930 Ma-old granulite from Mount Sones, Enderby Land, Antarctica

L.P. Black[1], I.S. Williams[2] and W. Compston[2]

[1] Bureau of Mineral Resources, P.O. Box 378, Canberra, A.C.T., Australia
[2] Research School of Earth Sciences, Australian National University, G.P.O. Box 4, Canberra, A.C.T., Australia

Abstract. Ion microprobe U–Th–Pb analyses of zircons from a granulite-grade orthogneiss from Mount Sones, Enderby Land, Antarctica, record the ages of four principal events in the history of the gneiss, three of which already have been recognized through previous isotopic dating of other samples. The structure of the zircons indicates at least four different stages of growth. The several zircon ages were obtained by grouping the analyses according to the stage they represented in the observed "stratigraphic succession" of growth and thereby defining separate U–Pb discordance patterns for each stage. The stratigraphically oldest zircon (rare discrete cores) is indistinguishable in age from the most common, euhedrally zoned zircon. Both crystallized when the tonalitic precursor of the orthogneiss was emplaced into the crust 3927 ± 10 Ma ago, making the orthogneiss currently the oldest known terrestrial rock. The outer parts of most grains and some whole grains recrystallized at $2948 + 31/-17$ Ma, during or immediately after possibly ~100 Ma of high granulite grade metamorphism. The recrystallized zircon was isotopically disturbed by tectonism associated with reactivation of the southern margin of the Napier Complex at ~1000 Ma. In the intervening time, at 2479 ± 23 Ma, the cores and zoned zircon suffered a major isotopic disturbance involving movement of radiogenic Pb which left most of the crystals with radiogenic Pb deficiencies, but produced local radiogenic Pb excesses in others. A new generation of zircon, characterized by very high Th/U and low U, grew at that time. That event – deformation and possibly a minor rise in temperature – produced widespread perturbations of other isotopic systems throughout the Napier Complex.

Introduction

The geological history of the Archaean Napier Complex in Enderby Land, Antarctica (Fig. 1) is long and complicated, making determination of the geochronology of the region difficult and leading to some dispute over the interpretation of the many "ages" that have been measured.

The report of Pb–Pb ages ≥4000 Ma measured on enderbites and granulites from the Fyfe Hills (Sobotovich et al. 1976) was received with caution (Grew and Manton 1979) but it has stimulated a number of geochronological studies which have confirmed that some components of the Napier Complex date from the very earliest Archaean, although there is disagreement over details.

In this paper we report ion microprobe U–Th–Pb analyses of zircons from a granulite grade orthogneiss from Mount Sones, 100 km ENE of Fyfe Hills, and compare the results with other isotopic data on that and related rocks. The work was undertaken after conventional U–Pb analyses of the same zircon population had shown evidence that there was more than one generation of zircon in the rock and that the oldest zircons may be older than 3700 Ma (Black and James 1983).

The Napier Complex

The geological history and geochronology of the Napier Complex have been reviewed by a number of authors. The most recent summary and references to earlier work are given by Harley and Black (1986).

The Napier Complex is a major Archaean granulite terrain that was subject to high pressures and extremely high temperatures, probably for an extended period of time, relatively early in its history. The Complex is composed of layered gneisses of both igneous and sedimentary derivation and more predominant, relatively massive orthogneisses. The orthogneisses are mostly diopside normative and are further distinguished from the paragneisses by their trends on Q–Ab–Or, Ab–Or–An, FMA and SiO_2 variation diagrams (Sheraton and Black 1983). In the few cases where the contact between the layered and massive gneisses is not obscured by deformation, the latter appear to be intrusive into the former.

Three principal episodes of regional deformation and metamorphism have been recognized (Sheraton et al. 1980). D_1, M_1 involved tight isoclinal and recumbent folding at very high granulite grade (950° C, 0.7–1.0 GPa). Peak granulite facies conditions possibly were maintained until D_2, a second period of isoclinal folding. The Complex then cooled nearly isobarically to ~700° C, followed by D_3, open dome and basin folding, possibly accompanied by a slight pressure increase and thermal pulse.

The timing of the episodes of deformation and metamorphism is controversial and each episode need not necessarily have been synchronous throughout the Complex. One of us (LPB) has argued for several years that D_1 occurred approximately 3,070 Ma ago. This contention is based on the following: first, zircon U–Pb analyses and an imprecise Rb–Sr whole-rock isochron for paragneiss from Mount Sones (Black and James 1979), secondly, zircon U–Pb, a Rb–Sr whole-rock isochron (Black et al. 1983a) and a Sm–Nd whole-rock isochron (McCulloch and Black 1984) for felsic orthogneiss at Fyfe Hills and thirdly, a Rb–Sr whole-rock isochron for syn-tectonic felsic orthogneiss from Proclamation

Offprint requests to: L.P. Black

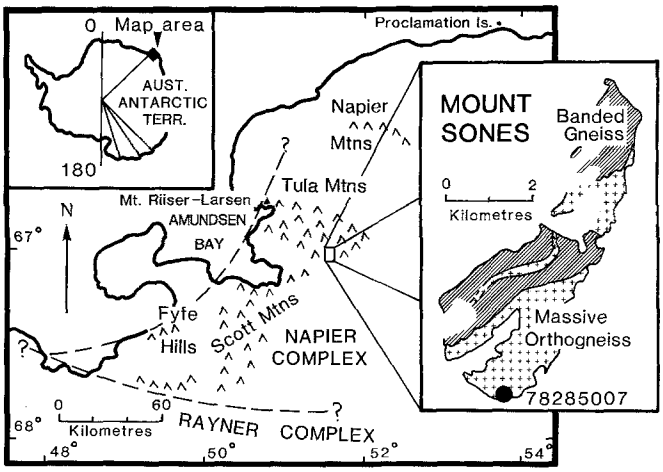

Fig. 1. Locality and sketch geological map of Mount Sones

Table 1. Chemical composition of Mount Sones orthogneiss 78285007

Major elements (weight percent)		Trace elements (micrograms per gram)			
SiO_2	66.9	V	20	Ba	659
TiO_2	0.42	Cr	7	La	61
Al_2O_3	16.9	Ni	9	Ce	90
Fe_2O_3	0.55	Cu	6	Pb	11
FeO	2.48	Zn	39	Th	3
MnO	0.02	Ga	17	U	0.5
MgO	0.88	Rb	31	As	0.5
CaO	3.81	Sr	323	Nd	29
Na_2O	5.18	Y	5	Sc	3
K_2O	1.95	Zr	183	Li	16
P_2O_5	0.13	Nb	8	Be	3

Analyst: J.W. Sheraton

Island (Sheraton and Black 1983). The age of D_2 has been harder to establish because it did not involve the development of a pervasive fabric. Black and James (1983) argue principally on the basis of zircon data from Mount Riiser-Larsen and Fyfe Hills that D_2 occurred about 2,900 Ma ago. In contrast, other workers have suggested that the major granulite facies metamorphism of the region took place about 2,500 Ma ago (Grew and Manton 1979; De Paolo et al. 1982), the age attributed to the geologically relatively minor, but isotopically pervasive, D_3 event by Black et al. (1983a, 1984) and McCulloch and Black (1984).

Mount Sones orthogneiss

Mount Sones in the Tula Mountains, E of Amundsen Bay (51°28′E, 67°02′S). Because the area has been examined only as part of a regional study, no detailed geologic map is available for the mountain. Mount Sones (20 km^2) is composed dominantly of strongly layered ortho- and paragneisses, except in the SE which is mainly orthogneiss (Fig. 1). The relative stratigraphic ages of the ortho- and paragneisses at Mount Sones are not known because contacts have been obscured by the intense D_1 and D_2 deformations.

The sample collected for zircon analysis was an orthogneiss of transitional granodioritic – tonalitic composition (78285007, Black and James 1983). A chemical analysis by J.W. Sheraton (*pers. comm.* 1983) is listed in Table 1. The orthogneiss is one of the suite of heavy REE-depleted orthogneisses recognized by Sheraton and Black (1983). Such orthogneisses probably represent new continental crust generated by the hydrous partial melting of amphibolite or garnet amphibolite. Rb–Sr and Sm–Nd analyses of the same orthogneiss and samples of other rock types from widely separated sites elsewhere on the mountain are reported by Black and McCulloch (in prep.).

Ion microprobe analytical procedure

Details of the procedure for determining U–Th–Pb in zircon using the ion microprobe SHRIMP have been given by Compston et al. (1984) and Williams et al. (1984). Briefly, handpicked and sized zircons were mounted in epoxy and polished to half their width to expose their centres. The mount was carbon coated. SHRIMP was operated at a mass resolution exceeding 6500 in order to eliminate all significant isobaric interferences. Potential remaining lead hydride interferences were monitored using a standard zircon of known $^{207}Pb/^{206}Pb$, and were negligible ($PbH^+/Pb^+ < 0.8\%$). Positive secondary ions sputtered from areas ≤ 40 μm diameter by an 11 kV primary beam of negative oxygen ions were measured by ion counting using a single collector. Zr_2O^+, $^{204}Pb^+$, background, $^{206}Pb^+$, $^{207}Pb^+$, $^{208}Pb^+$, $^{238}U^+$, ThO^+ and UO^+ were measured cyclically by magnetic field stepping. Pb isotopic ratios were measured directly and not corrected for mass discrimination, which was negligible. Elemental concentrations and interelement ratios were measured relative to a standard zircon (SL3) of known isotopic composition, constant (within 2% Pb/U and Pb/Th, and approximately constant (within 20%) uranium content. Progressive changes in Pb^+/U^+ and Pb^+/ThO^+ during the sputtering of each area were compensated for using a quadratic relationship between Pb^+/U^+ and UO^+/U^+ determined on the standard zircon. Systematic small changes in the relationship were monitored by interposing analyses of the standard with those of the sample zircons.

Analyses of the Mount Sones zircons

Zircons from Mount Sones orthogneiss 78285007 were originally analysed conventionally for U–Pb by Black and James (1983) who distinguished two distinct groups of zircons in the rock on the bases of colour, morphology and internal structure. Most of the crystals were brown, subhedral and markedly zoned; a minority were pale pink, transparent, relatively equant and optically homogeneous. Multi-grain analyses of six size fractions of the brown zircon showed only a small range in Pb/U and were highly discordant. A single analysis of a concentrate of the pink crystals showed a much lower U content, higher Th/U, and lower Pb/U and radiogenic $^{207}Pb/^{206}Pb$. Black and James' (1983) interpretation of this obviously multicomponent mixture was that the brown zircons could be about 3,700 Ma old and disturbed isotopically about 2,500 Ma ago, although a considerable extrapolation of a poorly-defined discordance line was required.

The same grouping by colour was made in preparing the zircons for the present ion microprobe analytical work. Pink, structureless zircons were hand picked from the population and the remaining zircons then subdivided into a number of magnetic fractions using an isodynamic separator. Selected fractions were prepared as two grain mounts, numbered 58 and 80.

The ion microprobe analyses were made during four sessions of two to five days each over a six week period. The work was interspersed with analyses of other samples for other elements and due to changes in probe operating conditions the data obtained are of different precision.

Session 1 involved a large number of reconnaissance and detailed analyses of mount 58. The primary ion current

used for the session was high, giving a high sensitivity (~35 counts/s/ppm for each Pb isotope) and therefore high precision in the measurement of the Pb isotopic composition. However control over inter-element fractionation was poor, leading to imprecise determinations of Pb/U and Pb/Th (4% coefficient of variation per set) and an underestimation of Pb, U and Th concentrations. After session 1 mount 58 was repolished.

Sessions 2 and 4 involved detailed analyses of grains on mount 58, some of which were reanalyses of areas analysed either in reconnaissance or detail during session 1. To distinguish the reanalyses from the originals, all analyses made after polishing have been identified with the suffix 'B'. The reanalyses cannot strictly be considered as duplicates of the earlier determinations because given the fine scale of zoning in the zircons, the removal of the surface of the grains during repolishing could easily have exposed zircon of different composition. Session 3 involved detailed analyses of mount 80.

For sessions 2, 3 and 4 a smaller primary ion current was used, resulting in reduced sensitivity (~8 counts/s/ppm for Pb) and a consequent reduced precision in the measurement of the Pb isotopic compositions. However, because the primary beam density was less and the rate of sputtering was lower, control over interelement fractionation was better, giving a precision of 1.8% per set in the determination of Pb/U and Pb/Th. Estimates of Pb, U and Th concentrations were accurate to within the range in uranium concentration in the standard zircon (20%).

The analyses are listed in Table 2. In the majority of cases one analysis is listed for each spot. That analysis is the mean of two or three determinations, each based on one data set) seven cyclic measurements of the relevant ion beams). Where there was a significant change in the composition of the zircon as the spot deepened (for example spot 58/51-2), successive analyses based on individual data sets have been listed instead. The tabulated uncertainties in Pb isotopic compositions and interelement ratios are counting errors calculated from the ion count rates combined, where appropriate, with the uncertainty in interelement ratio calculated from the interspersed analyses of the standard zircon. While it is our experience that the observed within-set precision for the analysis of a uniform target is consistent with that predicted by counting statistics, the listed uncertainties must nevertheless be considered minimum uncertainties for each analysis. Uncertainties in ages quoted in this paper, unless stated otherwise, are 95% confidence limits.

Each analysis has been corrected for initial Pb using the measured $^{204}Pb/^{206}Pb$ and an initial Pb composition calculated from the evolving Earth model (Model III) of Cumming and Richards (1975) and the inferred age of each zircon population. A calculated composition was used because we do not know the composition of the labile Pb in the zircons' environment at the times of crystal growth and recrystallization. In any case, the zircons have such low initial Pb contents that the actual composition chosen has a negligible effect on the corrected Pb isotopic compositions. The radiometric ages have been calculated using the constants recommended by the Subcommission on Geochronology (Steiger and Jäger 1977).

The analyses are grouped according to the type of zircon sampled. The classification is based on visual examination of the crystals after analysis and is a good but not perfect subdivision in terms of contrasting isotopic characteristics. When the zircon population is considered as a whole, a clear 'stratigraphic' sequence of zircon growth can be recognized, although all growth stages are not necessarily represented in one crystal. The great majority of the grains consist predominantly of strongly euhedrally zoned zircon, composed, on the basis of their response to HF etching, of alternating layers of high- and low-uranium zircon 1 to 10 μm thick (Fig. 2a). In a very few crystals, the euhedrally zoned zircon discordantly overgrows a distinct, weakly-zoned or unzoned core (Fig. 2b). Unconformably overgrowing the zoned portions of most crystals is a mantle, commonly 10 to 30 μm thick, of unzoned or weakly-zoned zircon. In some cases the zoning in the mantle is a ghost of the zoning in the remainder of the crystal (Fig. 2c). Commonly the mantle projects into deep embayments in the zoned interior (Fig. 2d); in one case a small euhedral outgrowth is present on the mantle (Fig. 2e). The pink, structureless zircon occurs as discrete crystals (Fig. 2f).

In terms of U and Th concentrations these zircon types show some consistent compositional differences; isotopically each zircon type is distinct.

Figure 3 is a plot of U and Th concentrations measured at each spot, with the different types of zircon sampled identified. There is a wide range in U and Th concentrations and Th/U ratio. The volumentrically dominant euhedrally zoned parts of grains have an average U content over 1,000 ppm, well above the average igneous zircon U content, based on average igneous rock U contents (Rogers and Adams 1969), of roughly 500 ppm. The bulk of the zircon, therefore, shows no evidence for major U loss during the prolonged granulite facies conditions to which the rock has been subjected. U and Th concentrations in the cores and weakly zoned parts of grains are lower on average than in the strongly zoned areas, but the range in Th/U in all is the same, 0.1–0.7.

The overgrowths on the zoned zircon show the same wide range in U contents as the latter but a much more restricted range in Th/U, 0.2–0.35. This is about the average of the Th/U ratios found in the zoned areas, suggesting that the uncomformable overgrowths may represent a rehomogenization of the older zoned zircon, a conclusion supported by the presence of ghost zoning in some of the overgrowths and the irregular, embayed contacts between these two zircon types.

The pink structureless crystals are themselves clearly of two types. Three of the grains (80/4, 80/9 and 80/12) are simply low-U equivalents of the brown zircons and are indistinguishable from them isotopically. In Fig. 3 they are plotted with the brown zircons. The remaining structureless grains are a discrete population characterized by very low and constant U concentrations (all but one in the range 120 to 183 ppm) and by very high Th/U (1.24–3.40). So different are those zircons from the remainder of the population that they almost certainly represent newly-grown zircon rather than recrystallized older grains.

It is very difficult to distinguish in thin section between the different zircon types except by a probable bimodality in grain size. The brown zircons are relative large (>25 μm diameter, on average about 50 μm diameter) and are visibly structured. Almost all of the structureless grains are smaller than 15 μm. About 60% of all zircons are located at the boundaries of major mineral grains, whereas the fine, structureless zircons occur exclusively at grains boundaries and

Table 2. Isotopic analyses of zircons from orthogneiss 78285007, Mount Sones, Enderby Land, Antarctica

Grain-Spot	Conc (ppm) U	Th	Th/U	f%	$^{208}Pb^*/^{206}Pb^*$ ±1σ	$^{207}Pb^*/^{206}Pb^*$ ±1σ	$^{206}Pb^*/^{238}U$ ±1σ	$^{207}Pb^*/^{235}U$ ±1σ	$^{208}Pb^*/^{232}Th$ ±1σ	Apparent ages (Ma) 206/238	208/232	207/206
Cores												
Grain 58/7, spots 1, 1B, 2, 2B and 4 (Williams et al. 1984)												
58/9-1	671	188	0.28	0.2	0.0752±4	0.3783± 6	0.834±24	43.52±1.24	0.223±7	3910	4070	3825±3
58/9-1B	2047	404	0.20	0.0	0.0510±5	0.3940±10	0.809±15	43.97±0.82	0.209±4	3820	3840	3886±4
80/16-1	768	296	0.39	0.1	0.1022±8	0.3757±10	0.760±10	39.34±0.53	0.201±3	3640	3700	3815±4
Mixture of core and euhedrally zoned												
Grain 58/7, spot 5 (Williams et al. 1984)												
58/21-1	1628	443	0.27	0.1	0.0748± 6	0.2459± 7	0.497±20	16.84±0.68	0.136±6	2600	2590	3159± 5
58/21-1	1565	425	0.27	0.1	0.0743± 6	0.2896± 8	0.546±22	21.81±0.88	0.149±6	2810	2810	3416± 4
58/21-1B	1271	211	0.17	0.1	0.0453± 6	0.3382± 9	0.721± 9	33.63±0.45	0.197±4	3500	3630	3655± 4
80/3-1	961	338	0.35	0.7	0.1029±22	0.2765±16	0.593±11	22.61±0.45	0.173±5	3000	3230	3343± 9
80/3-1	959	342	0.36	0.6	0.1011±23	0.2917±18	0.645±12	25.93±0.52	0.183±5	3210	3390	3427±10
Euhedrally zoned												
Weakly zoned												
Grain 58/7, spot 3 (Williams et al., 1984)												
58/28-2B	416	92	0.22	0.2	0.0574±17	0.3523±17	0.750±10	36.41±0.52	0.195±7	3610	3600	3717±7
58/40-4B	1407	101	0.07	0.1	0.0182± 4	0.3494± 8	0.750±10	36.13±0.48	0.189±5	3610	3500	3704±4
58/47-1	557	256	0.46	0.1	0.1215± 5	0.3579± 6	0.753±21	37.16±1.06	0.199±6	3620	3670	3741±3
58/47-1B	661	407	0.61	0.1	0.1654±11	0.4243±13	0.901±12	52.71±0.72	0.242±4	4140	4380	3997±5
58/51-1	1048	326	0.31	0.0	0.0829± 2	0.4224± 4	0.773±22	45.02±1.28	0.206±6	3690	3790	3991±1
58/51-2	816	250	0.31	0.0	0.0755± 4	0.4098± 8	0.813±33	45.95±1.85	0.201±8	3840	3700	3945±3
58/51-2	821	253	0.31	0.0	0.0764± 4	0.4187± 8	0.826±33	47.68±1.92	0.205±8	3880	3770	3977±3
58/51-2	836	254	0.30	0.0	0.0758± 4	0.4220± 8	0.824±33	47.95±1.93	0.206±8	3880	3780	3989±3
58/51-2	872	256	0.29	0.0	0.0738± 4	0.3973± 8	0.790±32	43.29±1.75	0.199±8	3750	3660	3898±3
58/51-2B	1643	224	0.14	0.1	0.0394±11	0.3667±13	0.791±14	40.00±0.76	0.228±8	3760	4160	3778±5
58/51-2B	1451	190	0.13	0.1	0.0361± 8	0.4044±12	0.936±17	52.17±0.98	0.258±8	4260	4640	3926±5
58/51-3	888	275	0.31	0.0	0.0769± 3	0.4219± 5	0.846±24	49.21±1.40	0.211±6	3950	3870	3989±2
Strongly zoned												
58/2-2	926	366	0.39	0.0	0.1177± 2	0.3322± 4	0.688±20	31.50±0.90	0.205±6	3380	3770	3627±2
58/2-3	465	124	0.27	0.1	0.0698± 4	0.3035± 5	0.627±18	26.24±0.75	0.164±5	3140	3070	3488±3
58/9-2	1959	378	0.19	0.1	0.0536± 2	0.3454± 3	0.776±22	36.96±1.05	0.216±6	3703	3950	3687±1
58/9-2B	1407	150	0.11	0.2	0.0278±11	0.2450±12	0.549±10	18.56±0.36	0.143±7	2820	2710	3153±8
58/10-1	1893	739	0.39	0.1	0.1050± 2	0.3702± 4	0.819±23	41.83±1.19	0.220±6	3860	4020	3792±2
58/10-1B	3539	1663	0.47	0.1	0.1318± 3	0.3592± 4	0.836± 9	41.40±0.44	0.235±3	3920	4270	3747±2
58/24-1B[a]	3340	826	0.25	0.1	0.0683± 4	0.2193± 5	0.632± 8	19.10±0.25	0.174±3	3160	3240	2977±4
58/28-1B	1920	541	0.28	0.1	0.0816± 6	0.2854± 7	0.628± 8	24.69±0.33	0.182±3	3140	3380	3393±4
58/29-1B	2190	510	0.23	0.1	0.0634± 4	0.3177± 6	0.689± 9	30.16±0.40	0.188±3	3380	3480	3559±3
58/37-1B	3127	1054	0.34	0.1	0.0922± 4	0.3678± 5	0.870±11	44.12±0.57	0.238±3	4040	4320	3782±2
58/40-1B	1478	391	0.26	0.1	0.0695± 6	0.3863± 9	0.817±11	43.52±0.58	0.215±3	3850	3940	3857±4
58/40-2	889	341	0.38	0.0	0.1020± 3	0.3533± 5	0.726±21	35.36±1.01	0.193±6	3520	3570	3721±2
58/40-3	998	286	0.29	0.1	0.0790± 3	0.3258± 4	0.652±18	29.28±0.83	0.180±5	3240	3340	3597±2
58/42-1B	2343	965	0.41	0.0	0.1219± 3	0.3918± 5	0.972±12	52.51±0.68	0.288±4	4380	5110	3878±2
58/42-2	1173	638	0.54	0.0	0.1439± 3	0.3781± 4	0.809±23	42.17±1.20	0.214±6	3820	3920	3824±2
58/45-2	775	249	0.32	0.0	0.0926± 3	0.3292± 4	0.626±18	28.41±0.81	0.180±5	3130	3340	3613±2
58/45-2B	2551	1266	0.50	0.1	0.1283± 5	0.3420± 6	0.763±10	35.98±0.47	0.197±3	3650	3630	3672±3
58/49-1B[a]	2685	684	0.25	0.0	0.0697± 4	0.2245± 5	0.628± 8	19.44±0.26	0.172±2	3140	3210	3013±4
58/50-1	824	192	0.23	0.1	0.0627± 4	0.2619± 5	0.524±15	18.92±0.54	0.141±4	2720	2670	3258±3
58/50-1B	2745	768	0.28	0.1	0.0754± 3	0.3107± 5	0.701± 7	30.03±0.32	0.189±2	3420	3500	3524±3
58/52-1B	2238	578	0.26	0.0	0.0686± 4	0.2887± 6	0.648± 8	25.79±0.34	0.174±3	3220	3240	3411±3
58/53-1	1851	719	0.39	0.0	0.0996± 5	0.3967± 7	0.893±11	48.84±0.64	0.229±3	4110	4170	3897±3
58/61-1B	1422	925	0.65	0.0	0.1645± 6	0.3938± 8	0.979±13	53.16±0.71	0.248±3	4400	4480	3886±3
80/17-1	1033	245	0.24	0.3	0.0674± 7	0.3053± 8	0.677± 9	28.50±0.38	0.193±3	3330	3570	3497±4
80/18-1	984	658	0.67	0.1	0.1864± 8	0.2929± 9	0.609± 8	24.59±0.33	0.170±2	3070	3170	3433±5
80/19-1	2889	565	0.20	0.0	0.0527± 2	0.3158± 5	0.704± 9	30.65±0.40	0.190±3	3440	3520	3550±2
80/22-1	2325	584	0.25	0.1	0.0713± 3	0.3163± 5	0.671± 9	29.26±0.38	0.191±3	3310	3530	3552±2
80/24-1	2914	862	0.30	0.0	0.0794± 3	0.3054± 5	0.681± 9	28.68±0.37	0.183±3	3350	3400	3498±3

Table 2 (continued)

Grain-Spot	Conc (ppm) U	Conc (ppm) Th	Th/U	f%	$^{208}Pb^*/^{206}Pb^*$ ±1σ	$^{207}Pb^*/^{206}Pb^*$ ±1σ	$^{206}Pb^*/^{238}U$ ±1σ	$^{207}Pb^*/^{235}U$ ±1σ	$^{208}Pb^*/^{232}Th$ ±1σ	Apparent ages (Ma) 206/238	208/232	207/206
Mixture of euhedrally zoned and uncomformable overgrowth												
58/2-1	514	75	0.15	0.1	0.0365± 3	0.2462± 4	0.621±18	21.09±0.60	0.155±5	3110	2910	3161±3
58/39-2B	2999	1006	0.34	0.1	0.0925± 4	0.2191± 5	0.622± 8	18.79±0.25	0.171±2	3120	3190	2974±4
58/45-1B	1265	177	0.14	0.1	0.0363± 7	0.3208± 9	0.696± 9	30.79±0.42	0.180±4	3400	3350	3574±4
58/51-4	437	109	0.25	0.1	0.0651± 6	0.2675± 7	0.574±16	21.17±0.61	0.150±5	2920	2820	3291±4
58/51-4B	794	181	0.23	0.3	0.0618±15	0.2276±12	0.597± 8	18.73±0.27	0.162±5	3020	3030	3035±8
Unconformable overgrowths												
58/1-1	1499	523	0.35	0.0	0.0956± 2	0.2043± 2	0.591±17	16.65±0.47	0.162±5	2990	3030	2861± 2
58/1-2	332	67	0.20	0.1	0.0550± 4	0.2054± 5	0.559±16	15.83±0.45	0.153±5	2860	2880	2870± 4
58/8-1	858	247	0.29	0.1	0.0788± 3	0.2059± 4	0.560±16	15.90±0.45	0.153±4	2870	2880	2874± 3
58/24-2B	684	138	0.20	0.3	0.0562±20	0.2139±14	0.581± 8	17.14±0.26	0.163±6	2950	3050	2935±11
58/39-1	1130	345	0.30	0.0	0.0863± 2	0.1970± 3	0.494±11	13.42±0.31	0.139±3	2590	2630	2802± 3
58/45-1	362	90	0.25	0.1	0.0680± 8	0.2126± 8	0.490±14	14.36±0.42	0.133±4	2570	2520	2926± 6
58/48-2B	1091	316	0.29	0.3	0.0802±11	0.2132± 9	0.573± 7	16.84±0.24	0.158±3	2920	2960	2930± 7
58/51-5B	893	211	0.24	0.1	0.0615±14	0.2013±11	0.461± 6	12.80±0.19	0.120±3	2440	2290	2837± 9
58/60-1	2462	832	0.34	0.0	0.0924± 3	0.1936± 4	0.470±13	12.55±0.36	0.129±4	2480	2450	2773± 3
80/11-1	555	116	0.21	0.2	0.0521±12	0.2113±11	0.508± 7	14.80±0.22	0.127±4	2650	2420	2916± 8
80/25-1	590	178	0.30	0.0	0.0872± 7	0.2091±10	0.531± 7	15.31±0.22	0.154±3	2750	2890	2899± 8
Pink, structureless												
80/1-1	125	385	3.08	0.9	0.9656±110	0.1664±42	0.447± 6	10.26±0.31	0.140±3	2380	2650	2552±43
80/1-1R	120	408	3.40	1.6	0.9650±161	0.1544±61	0.450± 9	9.59±0.45	0.128±4	2400	2430	2395±67
80/2-1	183	227	1.24	0.4	0.3695± 69	0.1678±34	0.452± 6	10.46±0.28	0.134±3	2400	2540	2536±34
80/4-1[b]	667	60	0.09	0.2	0.0220± 9	0.3064±11	0.687± 9	29.02±0.40	0.168±7	3370	3140	3503± 6
80/5-1	132	258	1.95	0.8	0.4944± 73	0.2362±35	0.523± 7	17.03±0.37	0.132±3	2710	2510	3095±24
80/6-1	139	370	2.65	0.8	0.7545±103	0.1661±43	0.455± 6	10.42±0.32	0.130±3	2420	2470	2519±43
80/7-1	124	173	1.39	1.6	0.3938± 88	0.1556±41	0.438± 6	9.40±0.30	0.124±3	2340	2360	2408±45
80/8-1	146	210	1.44	0.9	0.4085± 67	0.1586±32	0.444± 6	9.71±0.25	0.126±3	2370	2400	2441±34
80/9-1[a]	360	101	0.28	0.3	0.0790± 20	0.2239±15	0.583± 8	18.00±0.28	0.164±5	2960	3070	3009±11
80/10-1	316	562	1.78	0.7	0.5038± 42	0.1606±19	0.453± 6	10.03±0.19	0.129±2	2410	2450	2462±20
80/12-1[b]	243	154	0.63	0.0	0.1579± 14	0.4108±15	0.889±10	50.35±0.59	0.221±3	4100	4040	3949± 6
80/15-1	177	305	1.72	0.8	0.4935± 61	0.1658±28	0.459± 6	10.49±0.24	0.132±3	2440	2510	2516±28

B Analysis after repolishing of grain mount; R Repeat analysis on same spot; * Radiogenic Pb; f% Percent common ^{206}Pb

[a] Isotopically same as overgrowths

[b] Isotopically same as euhedrally zoned

generally in small groups, further suggesting that they may represent a late episode of new zircon growth. This conclusion is consistent with the observation of Black et al. (1983b) that elsewhere in the Napier Complex (in the Field Islands) this type of zircon is associated with areas of maximum D_3 major-mineral recrystallization.

Isotopic data

The U–Th–Pb data for one of the most complex of the Mount Sones zircons, grain 58/7, have been discussed already by Williams et al. (1984) as an outstanding example of the local imbalances in the U–Th–Pb isotopic system that can result from ancient movement of radiogenic Pb relative to its parent elements. Data for that grain have not been relisted in Table 2, although they are included in the plots and discussion below.

To understand the isotopic data it is necessary to group the analyses according to the generation of zircon which each represents. The best grouping isotopically is very similar to that above based on visual criteria, with a few exceptions. To avoid unnecessarily complicating the discussion we have not plotted the analyses of areas which overlapped two types of zircon and which therefore represent mixed isotopic systems.

Cores. The data from the few cores are dominated by the analyses of the core of grain 58/7 which contains a large and varied excess of radiogenic Pb. The other cores analysed, from grains 58/9 and 80/16, are either concordant or slightly normally discordant. The data scatter no more than is expected from the analytical uncertainties (MSWD = 1.55) about a discordance line with Concordia intercepts of 2,225±135 Ma and 3,927±10 Ma (tσ) (Fig. 4).

Euhedrally zoned. The structural classification of 'euhedrally zoned' is not sufficient for the best interpretation of the isotopic data. Euhedrally zoned zircon constitutes the great bulk of the population and real differences between the isotopic characteristics of different types of zoned zircon are evident. Some zoned areas, for example spots 58/24-1B and 58/49-1B, show isotopic affinities with the overgrowths. Both those spots sampled severely structurally damaged zircon with very high U contents immediately adjacent to overgrowth zircon. Conversely, some of the overgrowths,

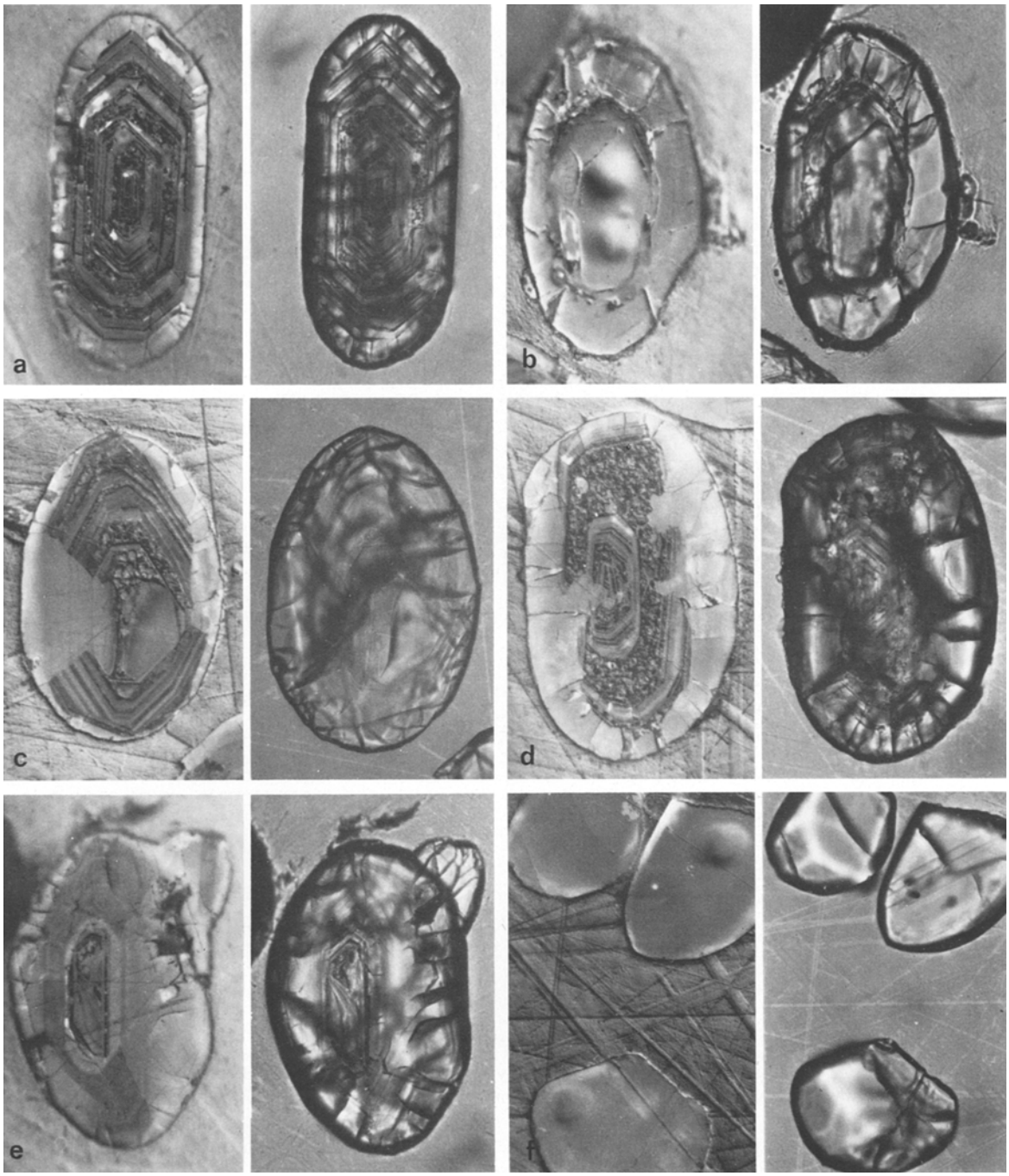

Fig. 2a–f. Photomicrographs illustrating structural features of the zircons from the Mount Sones orthogneiss (78285007). The photos are paired; one transmitted light and one normal reflected light with Normarski interference contrast. Fields of view are 200 × 300 μm. The zircons were etched for 20 s in HF vapour after analysis to accentuate their structures. **a** Grain 58/52, showing the strong euhedral zoning that is a feature of the great majority of the zircons. We interpret such zoning to be the product of magmatic crystallization. The thin structureless outermost layer is probably a ~3,000 Ma old mantle; it can be seen to crosscut the euhedral zoning, particularly at the ends of the crystal. Analysis 58/52-1B was made virtually in the middle of the crystal. **b** Grain 58/7. The grain consists of a structureless core overgrown by weakly euhedrally zoned zircon. No ~3,000 Ma old mantle appears to be present. The two pits sputtered during analyses 58/7-1B and -2B can be seen in the core. The core contains large and variable excesses of radiogenic Pb. The analysis of a single area on the weakly zoned outer layer (57/7-3) is slightly normally discordant at ~3,900 Ma. **c** An unanalysed grain from mount 80 showing strongly zoned zircon surrounded and deeply embayed by a mantle of recrystallized zircon. The mantle is considered to represent recrystallization rather than new zircon growth because it contains "ghosts" of the euhedral zoning which was present in the zircon it penetrates. **d** An unanalysed zircon from mount 80 showing strongly euhedrally zoned zircon surrounded and deeply embayed by a mantle of structureless zircon. The structureless zircon appears to have replaced the zoned zircon, rather than simply being an overgrowth on an older zoned grain. **e** Grain 58/48. The strongly-zoned centre of the grain is surrounded by weakly-zoned zircon, surrounded in turn by a thick structureless mantle which in places crosscuts the zoning. The small euhedral outgrowth on the mantle has the same isotopic features as the ~3,000 Ma old mantles on other grains and is evidence that some new zircon growth did occur at ~3,000 Ma. Analysis 58/48-2B was of the outgrowth only. **f** Structureless zircons, grains 80/12 (top right) and 80/15 (bottom). Areas where the grains were analysed are clearly visible as small pits. Like all the structureless zircons these grains are strongly rounded, transparent and relatively inclusion-free. The isotopic ages of the two analysed crystals are very different from one another; 80/15 is concordant at ~2,500 Ma, 80/12 is slightly reverse discordant at >3,900 Ma. Close inspection shows that 80/12 does in fact preserve a trace of euhedral zoning near its rounded end

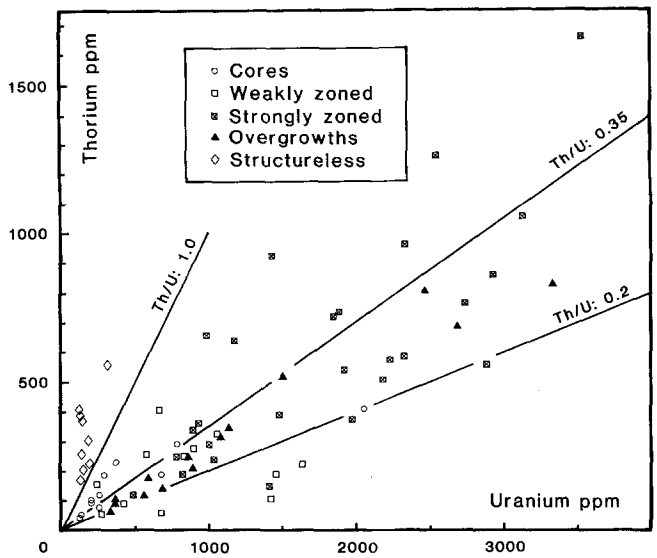

Fig. 3. Plot of uranium and thorium concentrations in the different types of zircon analysed illustrating 1, the low U and Th in the cores and weakly-zoned zircon 2. the high U and Th and variable Th/U in the strongly-zoned zircon. 3. the relatively constant and approximately average overall Th/U in the overgrowths 4. the distinctively high Th/U of the structureless grains, which is primarily a consequence of low U

for example at spots 58/60-1 and 80/11-1, still show weak remnant zoning. The remainder of the euhedrally zoned zircon can be divided into two groups, strongly zoned and weakly zoned. Within the weakly zoned group must be included grains such as 80/12 and 80/4 which show no zoning at all but which are isotopically unlike either the overgrowths or other structureless grains. The strength of the zoning reflects the presence or absence of zones of high U and/or Th content which are most structurally damaged and therefore most likely to have been open isotopically. Such a subdivision therefore separates areas likely to have been more disturbed from those like to have been less so.

The analyses of the euhedrally zoned areas, classified according to strength of zoning, are shown in Figs 5 and 6. Neither array of analyses defines a discordance line within analytical uncertainty, although there is a wide, real range in radiogenic $^{207}Pb/^{206}Pb$. The analyses of the weakly-zoned zircon mostly spread along the Concordia and give apparent ages up to, and even slightly above, the intersection age of the cores. Two of the analyses show reverse discordance (excess radiogenic Pb) similar to that in the core of grain 58/7. There is no evidence that the weakly-zoned zircon is significantly younger than the intersection age of the cores. The demonstrated presence of local excesses of radiogenic Pb due to *ancient* Pb movement makes it impossible to use the maximum $^{207}Pb/^{206}Pb$ age of the zoned zircon as an independent limit on its crystallization age, so we cannot presently attribute any geological significance to those $^{207}Pb/^{206}Pb$ ages which exceed 3,930 Ma.

The array of data for the strongly-zoned areas shows a very much wider dispersion in Pb/U with several points reversely discordant and most of the remainder strongly normally discordant. In view of the discordance pattern for the weakly-zoned areas it is not valid to place any direct age significance on the Concordia intersections of the array.

The combined discordance pattern for all the zoned zircon is consistent with it all having the same age as the cores (which represent the first zircon to crystallize in the rock), but with it having responded very differently to later isotopic disturbances. The dispersion in the analyses of the weakly-zoned zircon is due mainly to variable Pb loss during an early event, at about 3,000 Ma. The strongly-zoned zircon lost more Pb than the weakly-zoned during that event, then was strongly affected by another event about 500 Ma later.

Overgrowths. The analyses of overgrowths are isotopically very distinctive because they all fall on a short discordance array with a relatively limited range in radiogenic $^{207}Pb/^{206}Pb$ (Fig. 6). Analyses of zoned spots 58/24-1B and 58/49-1B and structureless spot 80/9-1 show the same isotopic characteristics.

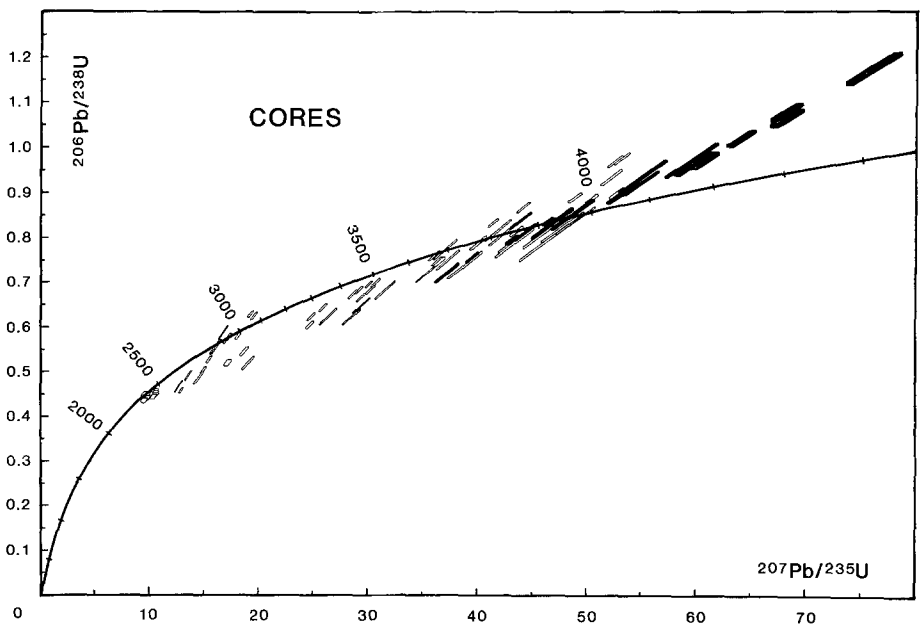

Fig. 4. Concordia plot of all zircon analyses from orthogneiss 78285007 with the analyses of zircon cores distinguished as filled symbols. Uncertainties are 1σ

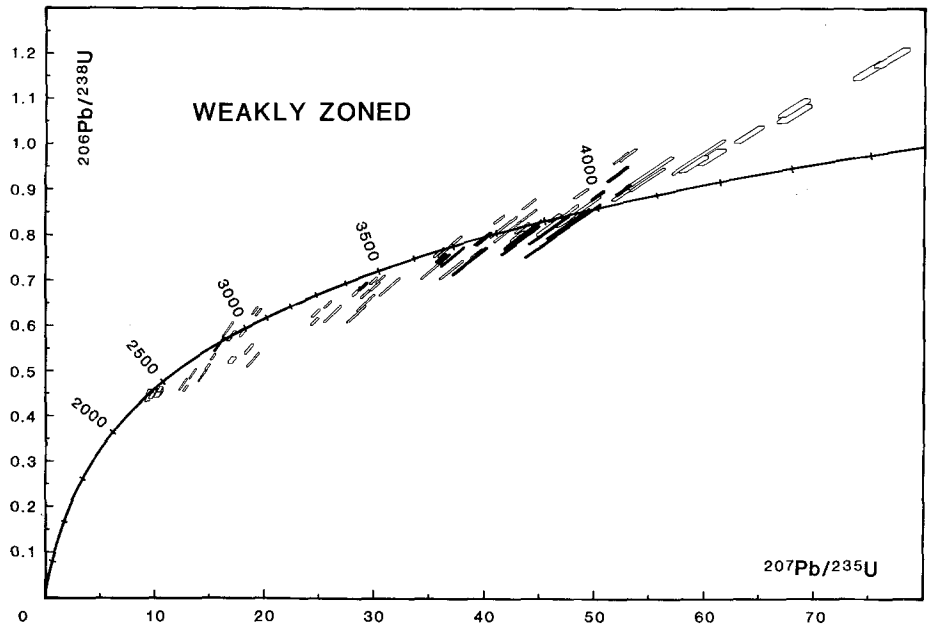

Fig. 5. Concordia plot of all zircon analyses from orthogneiss 78285007 with the analyses of weakly-zoned zircon distinguished as filled symbols. Uncertainties are 1σ

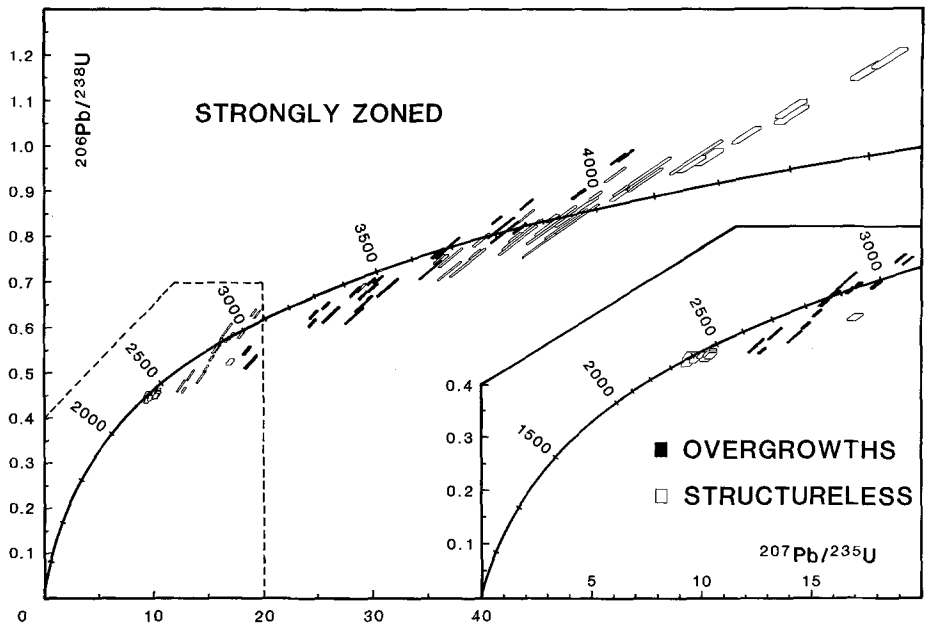

Fig. 6. Concordia plot of all zircon analyses from orthogneiss 78285007 with the analyses of strongly-zoned zircon distinguished as filled symbols. Inset shows analyses of the zircon overgrowths (*filled symbols*) and structureless grains (*open symbols*). Uncertainties are 1σ

The analyses do not define a single discordance line within analytical uncertainty (MSWD = 6.1). The Concordia intercepts calculated from a Model III (McIntyre et al. 1966) regression of the data are $1{,}310 \pm 460$ Ma and $2{,}948 \pm 31/-17$ Ma ($t\sigma$). If the three points that structurally are not overgrowths are excluded from the regression, the scatter is only marginally less (MSWD = 5.0) and the Concordia intercepts are not significantly changed, $1{,}040 \pm 670$ Ma and $2{,}919 \pm 62/-28$ Ma ($t\sigma$).

Structureless crystals. With the exception of those grains discussed above (80/4, 80/9 and 80/12) all the structureless grains analysed share the common compositional feature of having Th/U > 1.2, in marked contrast to all other zircons in the rock, for which Th/U < 0.7. With a single exception (grain 80/5), the U/Pb, Th/Pb and radiogenic $^{207}Pb/^{206}Pb$ ratios of the structureless crystals are respectively virtually identical. With the same exception, the U–Th–Pb analyses are almost concordant (Fig. 6). Despite the virtual concordance, determining the zircons' age is, in detail, subject to interpretation. On the one hand the zircons may be considered to have suffered minimal post-crystallization radiogenic Pb loss, in which case their age is most accurately given by their mean radiogenic $^{206}Pb/^{238}U$ as $2{,}394 \pm 20$ Ma (2σ). Alternatively the possibility of significant Pb loss can be taken into account and the age calculated from the mean radiogenic $^{207}Pb/^{206}Pb$ as $2{,}479 \pm 23$ Ma (2σ). The presence of old radiogenic Pb in one of the grains (80/5) argues for the first interpretation but, given that radiogenic $^{207}Pb/^{206}Pb$ in all the other grains is the same within analytical uncertainty and that the mean of the analyses is nevertheless not concordant,

we prefer the second interpretation. The best estimate of the age of the structureless zircons is therefore 2,479±23 Ma.

Geological implications of the isotopic data

Because of the large amount of isotopic and structural data which already has been obtained by earlier studies of the Napier Complex, the geological significance of the ion probe zircon U–Th–Pb analyses from the Mount Sones orthogneiss can be determined in very specific terms.

The oldest zircon in the rock is the cores, the analyses of which are well fitted to a discordance line with Concordia intersections of 2,225±135 Ma and 3,927±10 Ma. Because of the very real possibility that this line has not been generated by just one episodic disturbance of an old isotopic system, the lower intercept probably has no direct age significance. It does indicate however that the major isotopic disturbance of the cores occurred at or before 2,225±135 Ma. The same disturbance had a profound effect on the euhedrally zoned zircon that overgrows the cores, as is evidenced by the trend of the widely-dispersed array of data from the strongly zoned areas.

The fact that the disturbance at or before 2,225 Ma generated local excesses of radiogenic Pb both in the cores and zoned zircon complicates the interpretation of the data by removing the constraint on crystallization age normally imposed by $^{207}Pb/^{206}Pb$ apparent ages. The abnormal enrichment of ^{207}Pb in the excess Pb due to its early separation from its parent elements means that areas where excess Pb is present give $^{207}Pb/^{206}Pb$ apparent ages that geologically are *too old.*

To determine the minimum age for the cores it is therefore incorrect to use the maximum $^{207}Pb/^{206}Pb$ age measured. The most accurate age for the cores is given by the upper Concordia intersection of 3,927±10 Ma. This is neither a *minimum* nor a *maximum* age because the presence of ^{207}Pb-enriched excess Pb means that Pb loss could either increase or decrease the intersection age, depending upon whether it occurred after or before 2,225 Ma respectively. In reality Pb loss probably occurred during events both older and younger than 2,225 Ma but the fact the core analyses do fit to a discordance line within analytical uncertainty suggests, but does not prove, that their discordance is dominantly the result of one of those events and therefore that the intersection age of 3,927±10 Ma is a reliable measure of the true age.

We infer therefore that the bulk of the zircon is 3,927±10 Ma old. Because much of that zircon shows euhedral growth zoning with simple crystal forms the same as those found in zircons from many other rocks that are demonstrably igneous (prisms with length to width ratios >2 and simple pyramidal terminations) we consider 3,927±10 Ma to be a magmatic crystallation age, namely the time at which the tonalite that was later metamorphosed to form the Mount Sones orthogneiss was emplaced into the crust.

Black and McCulloch (in prep) report Sm–Nd and Rb–Sr whole-rock analyses of several orthogneisses from Mount Sones, including a number of samples from the 78285007 site. Because the orthogneiss is very uniform in chemical and isotopic composition, neither set of analyses precisely defines an isochron. Sr_{UR} model ages for the samples range from 5,900 Ma to 7,200 Ma. Similar impossibly-high Sr_{UR} model ages are found elsewhere in the Napier Complex and probably result from radiogenic Sr migration and/or Rb depletion during metamorphism (Sheraton and Black 1983; Sheraton et al. 1984). The Nd_{CHUR} model ages are more uniform, three samples giving 3,800 Ma, 3,850 Ma and 3,870 Ma. Considering that the orthogneiss protolith may actually have had a higher Sm/Nd than chondritic, these ages are strong support for a magmatic age greater than 3,870 Ma as we infer from the zircons.

If a ~2,225 Ma event were the only cause of discordance in the zoned zircon the analyses would be perfectly fitted to a straight line, but they are not. The scatter probably results from episodes of disturbance both before and after ~2,225 Ma, but it can be argued as follows from the pattern of discordance that it was an event substantially earlier than ~2,225 Ma that was the most important. It is to be expected that the weakly-zoned, relatively low U–Th zircon would be less isotopically disturbed by any event than the more U–Th-rich strongly-zoned zircon. This is borne out by the lesser response of the weakly-zoned zircon to the ~2,225 Ma event. If the dispersion in the analyses perpendicular to the trend imposed by the ~2,225 Ma event is considered, it is evident that the analyses of the weakly-zoned zircon are systematically higher in $^{207}Pb/^{206}Pb$ at any given $^{207}Pb/^{235}U$ than those of the strongly-zoned zircon. Assuming the weakly-zoned zircon to be the less isotopically disturbed, a pre-existing discordance at ~2,225 Ma, generated by a substantially earlier event is indicated. The range of the scatter shows that that earlier event must have been later than 3,600 Ma.

It is highly likely that the initial disturbance of the zoned zircon occurred close to the time that the zircons acquired their overgrowths. As discussed above, the analyses of the overgrowths, although scattered and showing in some cases a small amount of excess radiogenic Pb, form a coherent group with Concordia intersections of 2,948+31/−17 Ma and 1,310±460 Ma (Model III, McIntyre et al. 1966). The structure of the overgrowths (the commonly deeply embayed contacts with older zircon and the survival of ghost euhedral zoning) leaves little doubt that they are the result of recrystallization during metamorphism rather than being new zircon growth. An important exception is the overgrowth represented by spot 58/48-2B, which is a small euhedral outgrowth on a thickly mantled crystal (Fig. 2e). Some new zircon therefore did grow when the overgrowths formed.

The scatter in the array of overgrowth analyses potentially poses a problem in detailed interpretation because, accepting that they mostly represent recrystallized older zircon, some old radiogenic Pb might be expected to remain, making the Concordia intersection age only a *maximum* age for recrystallization. However, it can be argued that the overgrowths contain no older radiogenic Pb at all. The analysis of the newly-grown zircon at spot 58/48-2B is concordant at 2,930±14 Ma (2σ), not significantly younger than the Concordia intersection of the array. It is therefore likely that 2,948+31/−17 Ma is a *minumum* age for the overgrowths.

This age is indistinguishable from the age of ~2,900 Ma attributed by Black and James (1983) to the D_2 deformation which marked the beginning of isobaric cooling of the Napier Complex from high granulite grade; it is, however, significantly younger than the 3,070±34 Ma D_1 event (Sheraton and Black 1983, Rb–Sr whole-rock isochron)

which accompanied the onset of granulite facies conditions at Proclamation Island 150 km NE of Mount Sones. The 2,948 Ma age of the overgrowths may indicate that the partial recrystallization of the zircons was a consequence of enhanced element mobility caused by the D_2 deformation and not due to the granulite facies conditions as such. Alternatively, the recrystallization may have occurred throughout the prolonged granulite facies metamorphism, but the isotopic systems in the recrystallized zircon may not have closed until the time of D_2, when temperatures began to fall. A third possibility is that D_1 and the beginning of granulite facies metamorphism at Mount Sones occurred later than at Proclamation Island.

Given the possible duration of the granulite facies conditions (~100 Ma, Black and James 1983) and the total U–Th–Pb isotopic resetting in the zircon overgrowths, the relatively minor effect of the metamorphism on the zoned zircon and cores is remarkable. We can only suggest that volume diffusion in zircon is so slow that under dry conditions even ~100 Ma at temperatures of ~950° C is insufficient to homogenize crystals of ~150 μm diameter.

The lower Concordia intercept of the overgrowths' discordance line, 1,310±460 Ma, indicates Pb movement in that zircon phase even later than ~2,225 Ma. It could be argued that the ~1,300 Ma intercept is an artefact of early and recent losses of Pb. However, as the margin of the Napier Complex and the Rayner Complex to the south underwent high grade metamorphism (700° C, 0.7 GPa) and deformation ~1,000 Ma ago (Grew 1978; Black et al. 1983a, 1984), it is most likely that the discordance was caused by tectonism associated with that event.

The 2,479±23 Ma age of the structureless pink crystals is indistinguishable from the age of pervasive isotopic resetting throughout the Napier Complex during the D_3 deformation, 2,456+8/−5 Ma (Black et al. 1983b). The high Th/U in those crystals (>1.2) is so different from that (<0.7) in all the other orthogneiss zircons (due to lower than average U contents rather than higher than average Th) that the structureless grains must have crystallized in a very different chemical environment from the cores, zoned zircon and overgrowths.

Zircons from igneous rocks usually show U and Th enrichments over their host rocks by factors of approximately 150–200 and 20 respectively (Silver et al. 1980). The average U and Th contents of about 1,200 and 400 ppm respectively for the older zircon therefore imply that the tonalitic precursor of the orthogneiss originally contained about 6 ppm U and 20 ppm Th. The present-day U and Th levels in the rock are much lower, 0.5 and 3 ppm respectively, showing that the orthogneiss has lost perhaps 90% of its U and 85 percent of its Th, with almost a doubling of its Th/U from ~3.3 to 6. Neither is the U–Th composition of the structureless crystals wholly consistent, by the above reasoning, with the orthogneiss's present U and Th levels. Their very low U contents and high Th/U suggest that although they grew after the U–Th loss occurred, they did so from a fluid, presumably of metamorphic origin, with a composition very different from that of the whole rock. By the same reasoning, the ~2,948 Ma old recrystallization occurred before that loss. Lack of alteration of the pyroxene in the orthogneiss and the scarcity of biotite indicates that the fluid was primarily non-aqueous.

One can speculate on the timing of the U–Th loss. The recrystallized areas show no evidence of having grown in a Th–U environment any different from that existing when the zoned zircon or cores grew. The implication is that the U–Th loss therefore occurred after 2,950 Ma ago, or that the zircons remained closed with respect to U and Th during recrystallization. The latter was probably not the case, for zircons from the Swedish Caledonides similarly recrystallized under granulite grade conditions show profound changes in Th/U (Williams and Claesson, in prep).

By ~2,480 Ma ago, when the structureless grains grew, the U–Th loss had occurred. Geochemically, the most likely time for Th–U movement would have been during dehydration of the protolith during the first major granulite grade event which began ~3,070 Ma ago. The implication of the zircon ages is that Th and U did not leave the rock until late in that event or possibly even after it.

The event that had the greatest effect on the zircon U–Pb systems was that ~2,500 Ma ago. In contrast, it was the 3,070±34 Ma event which most disturbed the whole rock Rb–Sr and Sm–Nd systems throughout the Napier Complex. It is not obvious why the ~2,500 Ma zircon growth occurred entirely as new crystals rather than also as mantles on pre-existing grains. One possibility is that the zirconium for the new growth was introduced by the metamorphic fluid discussed above and that the pre-existing zircons were shielded from the fluid as inclusions in the major minerals. Support for this argument is the interstitial occurrence of the structureless zircons. Evidence that the structureless zircons are not entirely new growth is the remnant of old radiogenic Pb in crystal 80/5, despite its strong chemical similarity to the pink structureless group.

Conclusions

U–Th–Pb isotopes in zircons from the Mount Sones orthogneiss record the times of four principal events in the history of the rock:

1. Emplacement of the tonalite magma at 3,927±10 Ma, when most of the zircon crystallized.
2. Cooling at 2,948+31/−17 Ma after possibly 100 Ma of high granulite grade metamorphism, during which there was extensive zircon recrystallization but little new zircon growth.
3. Element mobilization, resulting in the growth of new zircon, during deformation and a minor thermal pulse at 2,479±23 Ma.
4. Tectonism at ~1,000 Ma, which caused a small amount of zircon Pb loss.

The older isotopic systems in the zircons were relatively weakly affected by possibly 100 Ma of high granulite grade conditions between 2,950 and 3,070 Ma ago. They were however strongly affected by later lower-grade metamorphism when there may have been movement of non-aqueous fluiuds.

An essential aspect of interpreting zircon analyses from polymetamorphic rocks is the recognition of the multiple stages of zircon growth in the rock and the definition of the individual discordance patterns for each stage.

Acknowledgements. Logistic support for L.P. Black in Enderby Land was provided by the Antarctic Division, Department of Science. We thank Dr. M. Grünenfelder for his constructive review of the manuscript and Drs. J.W. Sheraton and R.J. Tingey for their comments on the text. The contribution of L.P. Black is

published with the permission of the Director, Bureau of Mineral Resources, Geology and Geophysics, Canberra.

References

Black LP, James PR (1979) Preliminary isotopic ages from Enderby Land, Antarctica. Geol Soc Aus J 26:266–267 (Abstract)

Black LP, James PR (1983) Geological history of the Archaean Napier complex of Enderby Land. In: Oliver RL, James PR, Jago JB (eds) Antarctic Geoscience. Australian Academy of Science Canberra, pp 11–15

Black LP, James PR, Harley SL (1983a) The geochronology, structure and metamorphism of early Archaean rocks at Fyfe Hills, Enderby Land, Antarctica. Precamb Res 21:197–222

Black LP, James PR, Harley SL (1983b) Geochronology and geological evolution of metamorphic rocks in the Field Islands area, East Antarctica. J Metamorphic Geol 1:277–303

Black LP, Fitzgerald JD, Harley SL (1984) Pb isotopic composition, colour and microstructure of monazites from a polymetamorphic rock in Antarctica. Contrib Mineral Petrol 85:141–148

Compston W, Williams IS, Meyer C (1984) U–Pb geochronology of zircons from lunar breccia 73217 using a sensitive high mass-resolution ion microprobe. Proc Lunar Planet Sci Conf 14th, J Geophys Res 89 [Suppl] B525–534

Cumming GL, Richards JR (1975) Ore lead isotope ratios in a continuously changing earth. Earth Planet Sci Lett 28:155–171

DePaolo DJ, Manton WI, Grew ES, Halpern M (1982) Sm–Nd, Rb–Sr and U–Th–Pb systematics of granulite facies rocks from Fyfe Hills, Enderby Land, Antarctica. Nature 298:614–618

Grew ES (1978) Precambrian basement at Molodezhnaya station, East Antarctica. Bull Geol Soc Am 89:801–813

Grew ES, Manton WI (1979) Archaean rocks in Antarctica: 2.5 billion year uranium lead ages of pegmatites in Enderby Land. Science 206:443–445

Harley SL, Black LP (1986) The Archaean geological evolution of Enderby Land, Antarctica. In: Tarney J, Park RG (eds) Proceedings of conference on the evolution of the Lewisian and comparable Precambrian terrains. Leicester Univ, UK

McCulloch MT, Black LP (1984) Sm–Nd isotopic systematics of Enderby Land granulites and evidence for redistribution of Sm and Nd during metamorphism. Earth Planet Sci Lett 71:46–58

McIntyre GA, Brooks C, Compston W, Turek A (1966) The statistical assessment of Rb–Sr isochrons. J Geophys Res 71:5459–5468

Rogers JJW, Adams JAS (1969) Uranium, Abundances in common igneous rocks. In: Wedepohl KH (ed) Handbook of Geochemistry. Springer, Berlin Heidelberg New York, pp 92-E-1-92-E-8

Sheraton JW, Offe LA, Tingey RJ, Ellis DJ (1980) Enderby Land, Antarctica – an unusual Precambrian high-grade metamorphic terrain. J Geol Soc Aust 27:1–18

Sheraton JW, Black LP (1983) Geochemistry of Precambrian gneisses: relevance for the evolution of the East Antarctic shield. Lithos 16:273–296

Sheraton JW, Black LP, McCulloch MT (1984) Regional geochemical and isotopic characteristic of high-grade metamorphics of the Prydz Bay area: the extent of Proterozoic reworking of Archaean continental crust in East Antarctica. Precamb Res 26:169–198

Silver LT, Williams IS, Woodhead JA (1980) Uranium in granites from the southwestern United States: Actinide parent-daughter systems, sites and mobilization. First year rept for Dept of Energy, DOE-GJBX-45(81), Calif Inst of Technology, pp 379

Sobotovich EV, Kamenev YeN Komaristyy AA, Rudnick VA (1976) The oldest rocks of Antarctica (Enderby Land). Int Geol Rev 18:371–388

Steiger RH, Jäger E (1977) Subcommission on Geochronology: convention on the use of decay constants in geo- and cosmochronology. Earth Planet Sci Lett 36:359–362

Williams IS, Compston W, Black LP, Ireland TR, Foster JJ (1984) Unsupported radiogenic Pb in zircon: a cause of anomalously high Pb–Pb, U–Pb and Th–Pb ages. Contrib Mineral Petrol 88:322–327

Received March 12, 1986 / Accepted August 22, 1986